

## Optimum process condition determination for the treatment of Disperse Blue 60 dye by electrocoagulation with Taguchi method

Fuat Ozyonar<sup>a</sup>, Hamdi Muratçobanoğlu<sup>b</sup>, Ömür Gökkuş<sup>c,\*</sup>

<sup>a</sup>Department of Environmental Engineering, Sivas Cumhuriyet University, Sivas 58140, Turkey, email: fozyonar@cumhuriyet.edu.tr (F. Ozyonar)

<sup>b</sup>Department of Environmental Engineering, Niğde Ömer Halisdemir University, Niğde 51240, Turkey, email: hamdi.murat@ohu.edu.tr (H. Muratçobanoğlu)

<sup>c</sup>Department of Environmental Engineering, Erciyes University, Kayseri 38039, Turkey, email: omurgokkus@erciyes.edu.tr (Ö. Gökkuş)

Received 10 December 2019; Accepted 17 May 2020

### ABSTRACT

Wastewater produced in textile processes cannot meet the discharge standards especially in terms of color content and therefore, the treatment demand occurs. In many studies, electrocoagulation has been used in the removal of dyestuff. High removal efficiency, lower space requirement, and easy controllability are the main advantages of the EC process. In this study, removal of Disperse Blue 60 of 100 mg L<sup>-1</sup> by electrocoagulation with Taguchi method was investigated. In the reactor, monopolar-parallel connected Al anode and stainless steel cathode were used as electrode materials. The initial pH, current density, and electrocoagulation time were optimized and the effects of these parameters on the dye removal were employed at conductivities values. The operational conditions for EC process according to Taguchi model were employed as conductivity values of 500; 1,000; and 1,500  $\mu\text{S cm}^{-1}$ , pH 5, 6, and 7, current density ( $j$ ) of 40, 80, and 100 mA cm<sup>-2</sup> and electrolysis time ( $t$ ) of 2.5, 5, and electrolysis time 10 min. The highest removal efficiency (99%) was attained with the conductivity of 500  $\mu\text{S cm}^{-1}$ , pH 6,  $j = 80$  mA cm<sup>-2</sup>, and  $t = 10$  min. However, only 34% of color were removed with the conductivity value of 500  $\mu\text{S cm}^{-1}$ , pH = 5 at  $j = 40$  mA cm<sup>-2</sup> and  $t = 2.5$  min.

**Keywords:** Electrocoagulation; Disperse Blue 60; Textile wastewater; Stainless steel electrode; Dye removal

### 1. Introduction

Textile industry uses massive volumes of water during dyeing and finishing processes and this water turns into basically dye and chemical polluted wastewater [1]. Due to reducing the light transmittance, limiting the photosynthetic activity of aqueous environment colored wastewater is one of the most important environmentally problems [2]. Furthermore, dyes and wastewater polluted with dyes can be mutagenic, toxic, and carcinogenic [3]. Many

biological, chemical, and physical conventional treatment processes such as adsorption, activated sludge, coagulation–flocculation, ozonation, Fenton, electrocoagulation [4–9] have been widely used to treat dye polluted wastewater. Among them, electrocoagulation has advantages like easy operate, high efficiency, low investment cost, fast reaction rate, compactness, and low excess sludge [10,11]. Basically, pollutants in soluble or colloidal forms are removed by adsorption mechanisms on hydroxide flocks formed by electrocoagulation. If aluminum and stainless steel are used as electrode

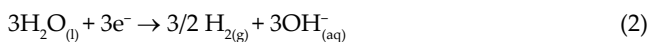
\* Corresponding author.

materials for anode and cathode, respectively, the following reactions take place:

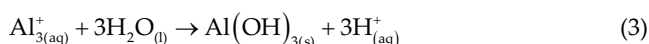
Anode:



Cathode:



By electrode reactions (1) and (2), the  $\text{Al}^{3+}$  and  $\text{OH}^{-}$  ions are generated and they react to form various monomeric species such as  $\text{Al}(\text{OH})^{+2}$ ,  $\text{Al}(\text{OH})_2^{+}$ ,  $\text{Al}_2(\text{OH})_2^{4+}$ ,  $\text{Al}(\text{OH})_4^{-}$  and polymeric species such as  $\text{Al}_6(\text{OH})_{15}^{3+}$ ,  $\text{Al}_7(\text{OH})_{17}^{4+}$ ,  $\text{Al}_8(\text{OH})_{20}^{4+}$ ,  $\text{Al}_{13}\text{O}_4(\text{OH})_{24}^{7+}$ ,  $\text{Al}_{13}(\text{OH})_{34}^{5+}$  and finally turn into a form of  $\text{Al}(\text{OH})_{3(s)}$  according to complex precipitation kinetics (reaction (3)) [12]. Therefore, different damages take place on the electrode surfaces and it causes some changes in their buoyancy properties [13]. Finally, the electrodes become more stable when is employed stainless steel employed as cathode material and this could also contribute to color or global TOC decay.



In addition, the gasses produced in the reactions as the form of  $\text{O}_2$  and  $\text{H}_2$  via reaction (4) is very active when they interact with a solid surface of the electrode materials.



Optimization of the process conditions is essential for treatment efficiency and cost of EC as in all other processes [14]. Conventional optimization process is time-consuming and costly due to testing all conditional probabilities [15,16]. In the meantime, the basic approach for classical optimization studies, to change levels for one factor and keep the others constant, remains incapable in revealing the optimal combination due to ignoring the interaction between levels [16]. Many optimization processes applied to EC like response surface methodology, artificial neural networks, adaptive neuro-fuzzy inference system, and Taguchi [17–19]. By using Taguchi technique, the time required in order to find the best conditions for a process significantly reduced for experimental investigation. This is important when examining the impact of multiple factors on performance as well as to examine the effect of individual factors to determine which factor has less or more impact [20].

When the related literature is considered, it can be seen that there are some electrochemical treatment studies with disperse blue dyes. However, the longer electrolysis time is required in those studies, since the experiments are conducted with low wastewater volume, and also the operating parameters are not optimized. For example, Ghernaout et al. [21] reported 99.9% color removal at 60 min of electrolysis time by using Al electrodes for treatment of DB 2 dye. In another study, Rivera et al. [22] achieved 90% color removal at 120 min of electrolysis time using  $\text{PbO}_2$  electrode

for treatment of blue dye. According to their results, the required operating time was quite long because of the operating parameters were not optimized. This study specifically focuses on the treatment of DB 60 in shorter electrolysis time using the Taguchi experimental method, which can be controlled by major operating parameters.

In this paper, Taguchi experimental design method was applied to determine optimum initial pH ( $\text{pH}_i$ ), conductivity, reaction time, and current density in the electrocoagulation process employing aluminum anode and stainless steel cathode in order to provide maximum dye removal. The main advantage of the Taguchi design method is the optimization of experimental parameters, such as pH, conductivity, reaction time, and current density, with very few controllable variables, compared to other optimization methods. In this way, required electrolyze time, treatment cost, and qualified personnel demand can be reduced considerably. In the Taguchi method, suitable orthogonal series are chosen depending on control factors and their number of levels. The signal-to-noise ratio (S/N) is employed in order to identify the relationship between the parameters and the responses, which are the primary optimum levels for the operating parameters.

## 2. Materials

Disperse Blue 60 (DB 60) was purchased from Sirma Chemistry in Istanbul, Turkey and it was used as synthetic pollutants without purification and prepared at a concentration of  $100 \text{ mg L}^{-1}$  in aqueous solutions. All the solutions used in the experiments were prepared with ultrapure water from the Elga Purelab system. The initial pH was always adjusted to the desired value with diluted 0.1 M NaOH or 0.1 M  $\text{H}_2\text{SO}_4$  solutions. The chemical structure and characteristic properties of the DB 60 dye are given in Fig. 1 and tabulated in Table 1, respectively.

### 2.1. Electrochemical cell

The electrocoagulation runs were performed in batch mode in a Plexiglas cell of 1,000 mL capacity by Al/SS electrode placed vertically in the electrochemical cell (Al electrodes as an anode, SS electrodes as cathodes) and distanced 20 mm between electrodes, submerged in the cell (Fig. 2). In EC experiments employed the electrodes that have made of aluminum and stainless steel material with dimensions of  $50 \times 70 \times 2 \text{ mm}$  (Al: 99.53%; Si: 0.12%; Fe: 0.25% for Al, C: 0.05%, Si: 0.029%, Mn: 1.27%, P: 0.0034%, S: 0.0025%, Ni: 10%, Cr: 16%, and Mo: 2.2% for SS) and were connected to monopolar parallel mode. The direct current was supplied by a digital DC power supply (Alpha 10A-50V) and equipped with galvanostatic operational options. The total effective surface area of the electrodes is  $210 \text{ cm}^2$ .

### 2.2. Experimental procedures

The EC trials were carried out at  $25^\circ\text{C}$  constant temperature by using a water circulator (VWR MX 7L R-20). Before each experiment, the electrodes were cleaned with acetone to remove the oxidized surface layer and then

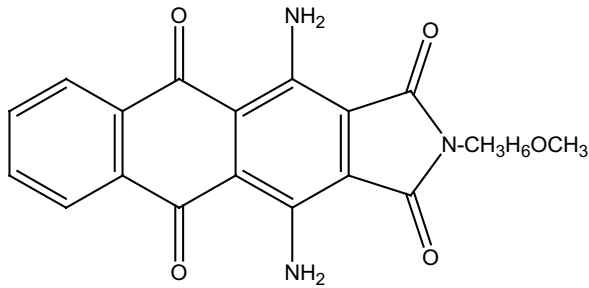


Fig. 1. Chemical structure of DB 60.

Table 1  
Chemical and physicochemical properties of DB 60

Parameter (Unit)	DB 60
Molecular Formula	C <sub>20</sub> H <sub>17</sub> N <sub>3</sub> O <sub>5</sub>
Molecular mass (g mol <sup>-1</sup> )	379.37
pH	6.5
Turbidity <sup>a</sup> (NTU)	40
Conductivity <sup>a</sup> (μS cm <sup>-1</sup> )	56
COD <sup>a</sup> (mg L <sup>-1</sup> )	150
TOC <sup>a</sup> (mg L <sup>-1</sup> )	28
λ <sub>max</sub> <sup>b</sup> (nm)	754

<sup>a</sup>Measurement was made with the dye concentration of 100 mg L<sup>-1</sup>.

<sup>b</sup>Determined from commercial DB 60 solutions at 25°C using a Merck Pharo 300 UV-vis spectrophotometer (Germany).

washed by dipping for 1 min into a solution freshly prepared by mixing 100 mL of HCl solution (35%) and 200 mL of hexamethylenetetramine aqueous solution (2.80%) [23]. The electrodes were rinsed with pure water on the electrode surfaces and then, dried at 70°C in the oven.

### 2.3. Analytical methods

The electrical conductivity and pH measurements were made with a Consort C-931 portable multi-parameter. The mineralization of aqueous solutions of DB 60 was assessed from the time course of TOC decay, measured by a TOC analyzer (Shimadzu, TOC-L). The dye concentration was measured with a Merck Pharo 300 UV-vis spectrophotometer (Germany) at λ = 754 nm wavelength. The COD measurement was determined using a spectrophotometrically (Merck Pharo 300 UV-vis, Germany) according to Standard Methods 5220-D closed reflux colorimetric method [24]. All experiments were made in parallel and average results have been considered. The removal percentages for color and TOC were calculated according to Eq. (5).

$$\text{The removal efficiency of color or TOC (\%)} = \frac{C_0 - C_t}{C_0} \times 100\% \quad (5)$$

where C<sub>0</sub> and C<sub>t</sub> are the concentrations (mg L<sup>-1</sup>) at an initial time and time t, respectively.

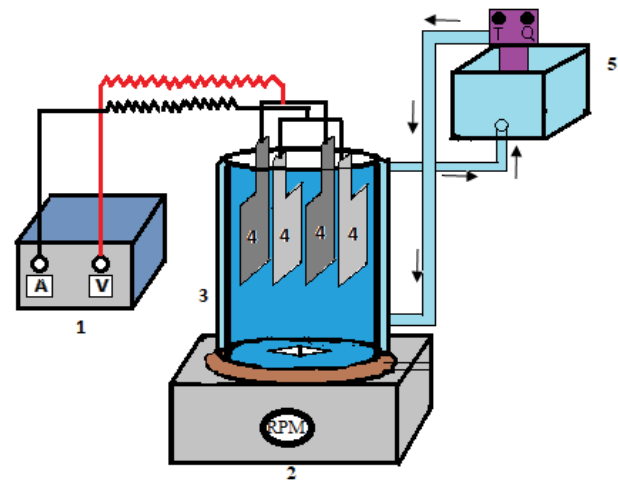


Fig. 2. Sketch of the electrochemical cell used for the EC treatment of DB 60 solutions. (1) Power supply, (2) magnetic stirrer, (3) EC reactor, (4) Al or SS electrodes, (5) water circulator.

### 2.4. Taguchi analysis

The four operational parameters (initial pH, current density, EC time, and electrical conductivity) were selected as variables in EC process. The Taguchi L9 (4<sup>3</sup>) OA experimental design, four variables with three parametric levels, was preferred as the most suitable method for the experimental design. The investigated parameters and their levels in EC have given in Table 2.

In the Taguchi design, signal-to-noise (S/N) ratio is the most known performance indicator. “The smaller is better,” “The nominal is better,” and “The larger is better” are frequently used S/N ratio functions. “The larger is better” is the maximum output value for the optimized process. The S/N ratios calculated with Eq. (6). The performance parameters in the Taguchi design using “The larger is better” were determined by the system performance in terms of COD, TOC, or color removal efficiencies.

The larger is better:

$$\frac{S}{N} = -10 \log_{10} \left( \frac{1}{n} \sum_{i=1}^n \frac{1}{Y_i^2} \right) \quad (6)$$

where n is the number of the experimental replication and Y<sub>i</sub> is the performance value of ith experiment.

Table 2  
Experimental variables and levels

Parameter	Level		
	1	2	3
A: pH	5	6	7
B: Current density (j) (mA cm <sup>-2</sup> )	40	80	100
C: Electrolysis time (min)	2.5	5	10
D: Electrical conductivity (μS cm <sup>-1</sup> )	500	1,000	1,500

### 3. Results and discussion

#### 3.1. Experimental results

The experiments were performed based on the Taguchi orthogonal array L9 matrix. Table 3 shows the experimental conditions and treatment results of DB 60 removal corresponding to the design matrix of four parameters with three levels by Taguchi.

The S/N ratio was employed to better understand the influence of each factor on color removal. The S/N ratio for a single factor can be calculated by averaging the value of S/N ratios at different levels. The mean S/N ratio for every factor was calculated and plotted in a graphical form. The peak points in these plots correspond to the optimum condition. The optimum conditions for color removal for EC process are shown in Fig. 3.

As can be seen in Fig. 3, the optimum levels that provided the best color removal were found as second (pH = 6), second ( $j = 80 \text{ mA cm}^{-2}$ ), third ( $t = 10 \text{ min}$ ), and second ( $\mu = 1,000 \text{ }\mu\text{s cm}^{-1}$ ) levels for the parameters pH, current density, electrolysis time, and conductivity, respectively.

#### 3.2. Effect of variables

##### 3.2.1. Effect of pH

In general, the solution pH plays a key role in the formation of insoluble metal coagulants as well as in the whole EC process. Several trials were conducted to reveal the effect of pH on the EC treatment of  $100 \text{ mg L}^{-1}$  of DB 60 solution according to Taguchi experimental matrix. Fig. 3 shows the highest S/N ratios depending on the investigated parameters like pH, current density, electrolysis time, and conductivity.

As depicted in Fig. 3, the highest S/N ratio, which means the best operational condition for pH, was achieved at pH 6, attaining 99% of color removal. High acidic pH values are not suitable for effective coagulation for pollutants. It is well-known that  $\text{Al}^{3+}$  and  $\text{OH}^-$  ions produced by the electrodes at pH values between 4 and 9 react to form several monomeric species like  $\text{Al}(\text{OH})_2^+$ ,  $\text{Al}(\text{OH})_2^{2+}$ , and polymeric species like  $\text{Al}_6(\text{OH})_{15}^{3+}$ ,  $\text{Al}_7(\text{OH})_{17}^{4+}$ ,  $\text{Al}_{13}(\text{OH})_{34}^{5+}$ , and finally are converted into insoluble amorphous  $\text{Al}(\text{OH})_{3(s)}$  through complex polymerization/precipitation reactions [25]. These species

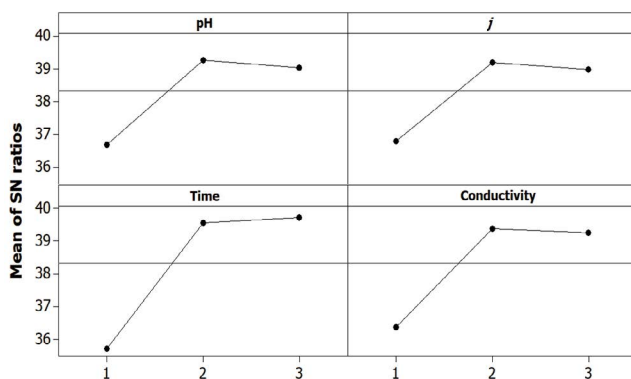


Fig. 3. S/N ratios vs. levels for the operational parameters such as pH, current density, time, and conductivity in EC treatment.

undergo complex polymerization and partly are converted into insoluble amorphous aluminum hydroxides, which have abundant surface hydroxyl groups for adsorbing heavy metal ions, and there are abundant hydroxyl groups on the surface area of these flocs, which have strong capability of dye adsorption [26]. Fig. 4 shows different  $\text{Al}(\text{OH})_3$  forms depending on the concentration of  $\text{Al}^{3+}$  ions and pH in the aqueous environment [27].

On the other hand, aluminum hydroxides which are the hydrolysis products of  $\text{Al}^{3+}$  are in soluble form at low initial pH value. Therefore, they cannot absorb the particles properly.  $\text{Al}(\text{OH})_2^{2+}$  and resulting  $\text{Al}(\text{OH})_2^+$  ions are the common cationic species from  $\text{Al}^{3+}$  hydrolysis reactions [28].

However, hydroxide ions produced at the cathode simultaneously causes an increase in the initial pH value of the wastewater during electrocoagulation. This increase is given in Table 3 for different experimental conditions and electrolyzes time. Along with metal hydroxide flocs formed at different pH values, pollutants can cause precipitation and co-precipitation. The sweep flocs formed are separated from the environment by precipitation and  $\text{H}_2$  flotation. As seen in Table 3, in the experiments in which the final pH values were 6–7, the pollutant removal efficiencies were higher than the other pH values. This can be explained by the fact that the  $\text{Al}(\text{OH})_3$  flocs formed predominate in this pH range. The minimum solubility pH value of solid  $\text{Al}(\text{OH})_3$  flocs is 6.5. The total soluble  $\text{Al}^{3+}$  concentration is  $3 \times 10^{-6}$ – $3 \times 10^{-4} \text{ M}$  (or  $0.025$ – $2.5 \text{ mg L}^{-1}$ ) in the pH range of 6–9 [29].

##### 3.2.2. Effect of current density

It is well-known that the applied current is a crucial operational parameter for any electrochemical process. To remove the color from DB 60 aqueous solution, monopolar, and parallel-connected Al anode and stainless steel cathode pairs were employed as electrode material in the electrolytic reactor. According to Fig. 3, the highest dye removal (99%) was achieved at the current density of  $80 \text{ mA cm}^{-2}$ , and then, a slight decrease was observed in color removal with raising the current density to  $100 \text{ mA cm}^{-2}$ . At higher current density ( $>80 \text{ mA cm}^{-2}$ ), the production of metal ions at the

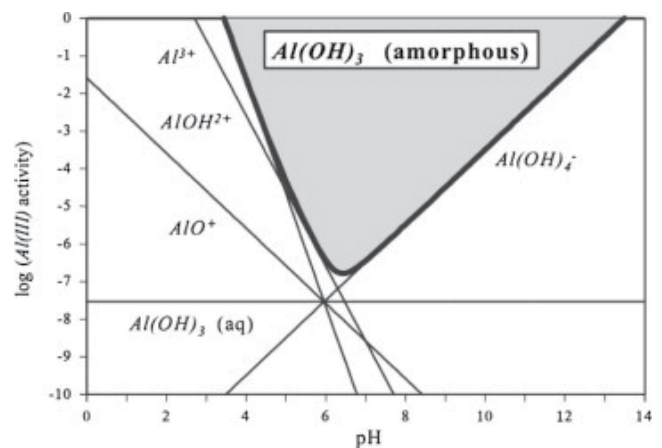


Fig. 4. Activity–pH relation for three valent aluminum species in equilibrium with  $\text{Al}(\text{OH})_3$  [27].

Table 3  
Independent variables and corresponding results

Run	Independent Variables						
	pH	Current density (mA cm <sup>-2</sup> )	Electrolyze time (min)	Conductivity (μs cm <sup>-1</sup> )	pH <sub>final</sub>	Color removal (%)	TOC removal (%)
1	5	40	2.5	500	5.35	33.75	34.19
2	5	80	5	1,000	5.89	98.13	93.42
3	5	100	10	1,500	6.45	96.00	94.45
4	6	40	5	1,500	6.98	98.50	96.65
5	6	80	10	500	6.85	95.13	89.55
6	6	100	2.5	1,000	6.75	82.75	72.13
7	7	40	10	1,000	8.01	99.13	96.77
8	7	80	2.5	1,500	8.14	81.50	67.61
9	7	100	5	500	8.32	88.88	78.06

anode was generated quicker than the coagulation process, causing a decrease in removal efficiency calculated on an equivalent aluminum or iron basis [30].

The amount of metal ion (iron or aluminum) released into solution by electrolytic oxidation of the anode material is a function of current and time and can be calculated using the following form of Faraday's law (Eq. (7)):

$$w = \frac{itM}{zF} \quad (7)$$

where  $w$  is the metal dissolved (g),  $i$  is the current (A),  $t$  is the contact time (s),  $M$  is the molecular weight of Fe or Al,  $z$  is the number of electrons involved in the redox reaction ( $z_{\text{Fe}} = 2$ ;  $z_{\text{Al}} = 3$ ), and  $F$  is the Faraday's constant (96,500 C/mol) [30]. Moreover, the bubble generation (oxygen and hydrogen) rate at both anode and cathode increases with current, which is beneficial for pollutants removed by flotation [31].

Fig. 5 illustrates the UV-vis spectra variation in the absorbance for DB 60 before and after EC treatment. Here, UV-vis spectra variations in absorbance for the initial and treated sample are used to monitor existing organic matter concentration in the medium [32]. The absorption peaks between 400 and 800 nm decreased and finally almost vanished after 10 min of EC treatment at a current density of 80 mA cm<sup>-2</sup>, indicating a rapid color removal. In addition, other peaks appeared in the UV band issued from by-products, and their intensities increased with the EC time. This phenomenon can be ascribed to the degradation of dye molecules leading to major absorbance peaks in the UV region of 250–380 nm, which are denoted to aromatic amines [32].

As seen in Fig. 5, DB 60 is characterized by two main peaks: a visible region with an absorbance peak at 754 nm, and an ultraviolet region with an absorbance peak at 292 nm. The peak at 754 nm belongs to chromophore or chromogen group –N=N– (azo bond) and the peak at 292 nm is related to benzene rings. Fig. 5 also illustrates that the peak at 754 nm abated quickly within 10 min and the absorbance was reduced to 0.015 from 0.289. This means the –N=N– was

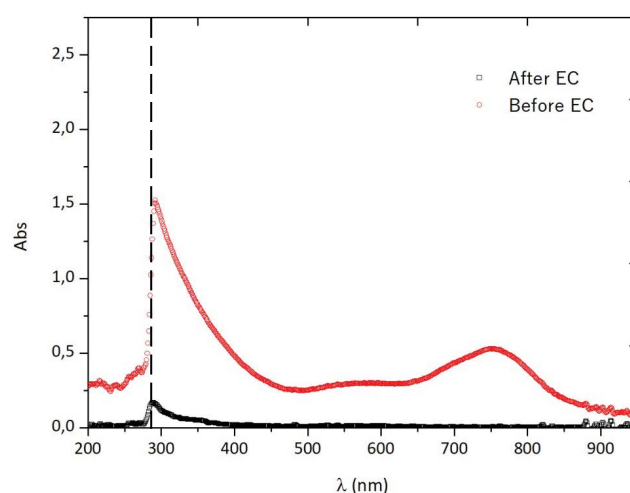


Fig. 5. UV-vis spectra changes along the EC treatment (before and after EC treatment of DB 60 of 100 mg L<sup>-1</sup> at the optimum conditions).

broken down after EC treatment, and the color was removed rapidly. As the EC treatment proceeds, the peak at 292 nm decreases concurrently with the reducing peak at 754 nm. During EC treatment, cleavage of –N=N– and aromatic rings occurred usually by means of anodic oxidation or chloride effect, resulting in a decrease of the absorbance band of the dye solution [31].

### 3.2.3. Effect of electrolysis time

Electrolysis time indicates the coagulant generation rate and total generation of coagulant (Al ions). Fig. 3 demonstrates the dye removal with electrolysis time depending on S/N ratio. As expected, the rise in electrolysis time provided more coagulant generation at the anode and thereby increased dye removal due to the promotion of electrocoagulation reactions (1) and (3).

To better understand the role of electrolysis time, a series of trials were carried out at 5, 10, and 15 min of electrolysis time with the Al/SS electrode pairs, and the

obtained results showed that the highest color and TOC removals were attained in 15 min of electrolysis time. This can be attributed to the anode dissolution. By increasing the electrolysis time, increased the flocs generation rate, and hence dye removal efficiency [33]. In addition, an increase in treatment time provided a longer contact time between the particles and coagulant agents so that increased the removal performance [34].

The removal trend is in a good agreement with the results presented by Shamaei et al. [34], who used EC to treat wastewater from oil sand produced water.

#### 3.2.4. Effect of electrical conductivity

The supporting electrolyte is used to increase the conductivity of the solution in order to reduce the resistance between electrodes. As resistance decreases, the cell potential decreases and contributes to the lesser power consumption during the EC treatment [31]. In the study, several trials have been carried out to investigate the effect of electrical conductivity on color removal during EC treatment. Dye solutions with different conductivities (500; 1,000; and 1,500  $\mu\text{S cm}^{-1}$ ) were electrolyzed at pH 6 and 80  $\text{mA cm}^{-2}$ . Fig. 3 shows the trend of the variation in S/N ratio, represents the removal rate, with the conductivity values ranging between 500 and 1,500  $\text{ms cm}^{-1}$ . As it can be seen, a conductivity value of more than 1,000  $\mu\text{S cm}^{-1}$  did not increase the color removal significantly.

Fig. 6 depicts the color removals under the different experimental runs according to Taguchi matrix. It is clearly seen that the best removal rate for color (99.1%) and TOC (96.8%) abatements were achieved with experiment (7) in the matrix.

Fig. 7 shows the color abatement in the dye solution of 100  $\text{mg L}^{-1}$  during the EC treatment period that almost the total color removal was reached at the optimum conditions.

The obtained results also showed that employing the EC process with Al/SS electrode pairs provided an effective decolorization and TOC abatement in a short treatment time after only 10 min. Fig. 8 shows the scanning electron

microscopy (SEM) images of the sludge samples belong to RR 241 and DB 60 dyes after EC treatment.

In order to reveal the difference between the final sludge formed by disperse and reactive dyes after EC treatment, the SEM analysis of the sludge shown in Figs. 8a and b was carried out. Fig. 8a points out the high crystallinity of the sludge covered with disperse dye after EC treatment. This can be explained by its insoluble structure in water. On the other hand, Fig. 8b shows that the reactive dye covered homogeneously on the flock surface due to its well-solubility in water.

#### 3.3. Effect of distance between electrodes

In the study, the effect of distance between electrodes was also examined apart from Taguchi model matrix. Fig. 9 illustrates the effect of the distance between the electrodes. In order to investigate the effect on color and TOC removal, the distance between the electrodes was changed in the range of 0.5–2 cm. As it can be seen in Fig. 9, the highest efficiency was obtained at a distance of 2 cm electrode.

In electrochemical processes, the distance between electrodes has a direct effect on the resistance between the anode and the cathode. If the distance between electrodes is too short, coagulation, flotation, and precipitation mechanisms can be adversely affected and the treatment efficiency may decrease. This can be explained as follows, due to the high electrostatic effect at a very short electrode distance, small particles are prevented from colliding, thus affecting the formation and precipitation of coagulation and flocculation.

#### 3.3. Operating cost analysis

Total operating cost consists basically of electrical energy, material (electrodes), maintenance, labor, and other costs [23,35]. The latter cost items were largely independent of the type of the electrode material. In the study, the total operating cost for the EC treatment was calculated from the electrode and electrical energy consumptions. Thus, the energy,

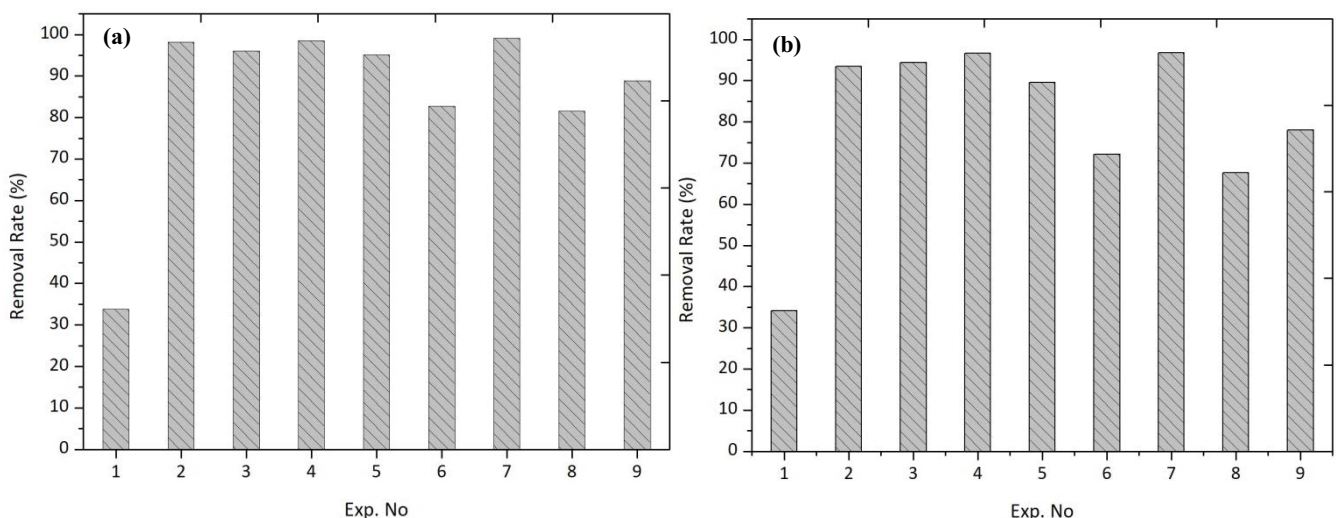


Fig. 6. (a) Color and (b) TOC abatements for EC treatment at the experimental conditions according to the L9 matrix.

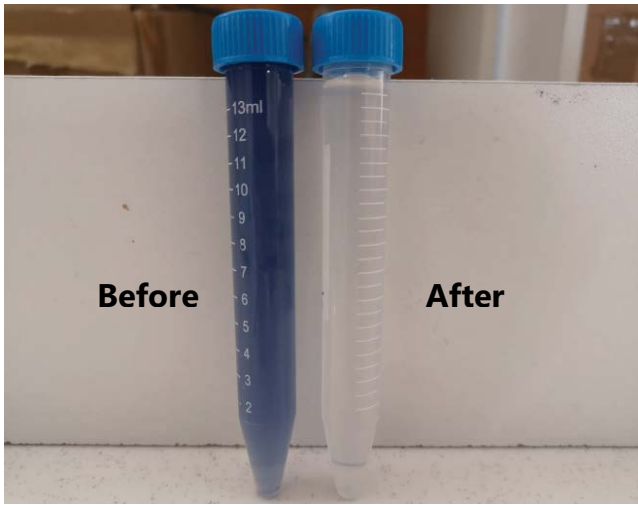


Fig. 7. DB 60 dye solution untreated (left) and treated (right) by EC process.

electrode, and chemical consumptions for the EC treatment were considered as the main cost items [36]. The total operating cost for the EC treatment was calculated according to Eq. (8).

$$\text{Operation cost for EC} = A \times C_{\text{energy}} + B \times C_{\text{electrode}} \quad (8)$$

where  $C_{\text{energy}}$  and  $C_{\text{electrode}}$  are consumption quantities,  $A$  is the electrical energy price (0.074 \$/kWh) and  $B$  is the electrode material price (1.7 \$/kg Al). Costs for electrical energy and electrode are calculated using Eqs. (9) and (10) [37,38]:

$$C_{\text{energy}} = \frac{V \times I \times t_{\text{EC}}}{\vartheta} \quad (9)$$

$$C_{\text{electrode}} = \frac{I \times t_{\text{EC}} \times Mw}{z \times F \times \vartheta} \quad (10)$$

where energy consumption is energy consumption (kWh  $m^{-3}$ ),  $V$  is voltage (Volt),  $I$  is current (Ampere),  $t$  is EC time (s), and  $\vartheta$  is the volume of the treated wastewater ( $m^3$ ),  $F$  is Faraday's constant ( $96485 \text{ C mol}^{-1}$ ), respectively. The energy consumption per kg of TOC removed is shown in Table 4.

In addition, current efficiency (CE) was calculated according to the ratio of the amount of experimentally released aluminum ion and theoretical release aluminum according to Eq. (11) [37,39,40].

$$\varnothing = \frac{ma}{\frac{I \times T_{\text{EC}} \times Mw}{z \times F}} \quad (11)$$

where  $ma$  is the actual mass of aluminum released into the solution was determined by weighing by taking the electrode mass difference before and after the EC experimental process.

The current efficiency of EC was between 95% and 119%. These results show that amounts of experimental aluminum released were more than theoretical aluminum. But, in experiments where electrical conductivity was  $1,500 \mu\text{S cm}^{-1}$ , the current efficiency was found to be low. The reason for this is the corrosion formed on the electrode surface due to  $\text{Cl}_2$ , which caused by excessive NaCl electrochemical reactions used to increase electrical conductivity. In this event, it may contribute to the passivation of the surface of the electrodes [41,42].

These findings indicate that the lowest operating costs were observed under the experimental conditions of the run 1 (Table 3), which is due to its lower current density ( $40 \text{ mA cm}^{-2}$ ) and shorter reaction time (2.5 min) compared to the others. However, the color and TOC were only reduced by 33.8% and 34%, respectively under these conditions. On the other hand, the highest operating cost values were observed under the experimental conditions of runs 3–5–8–9 (Table 3) and the confirmation experiment since that studies were conducted at higher  $j$  values ( $80$  or  $100 \text{ mA cm}^{-2}$ ) and longer electrolysis time (usually 5 or 10 min). It should be noted that the calculated operating cost under the conditions

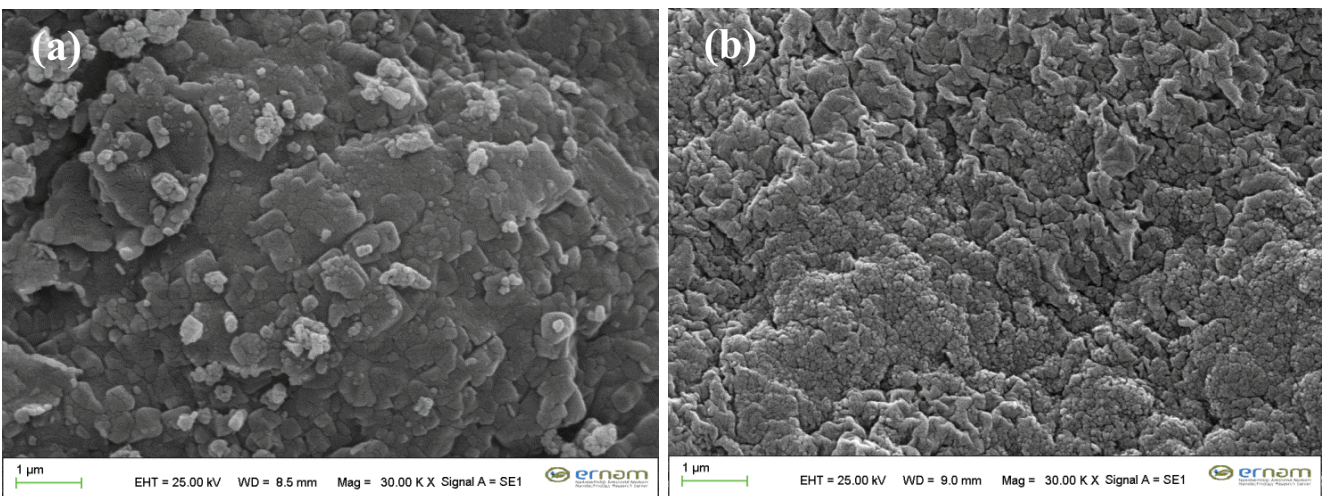


Fig. 8. SEM images of the final sludge samples after EC treatment for  $100 \text{ mg L}^{-1}$  of (a) RR 241 and (b) DB 60 dye solutions.

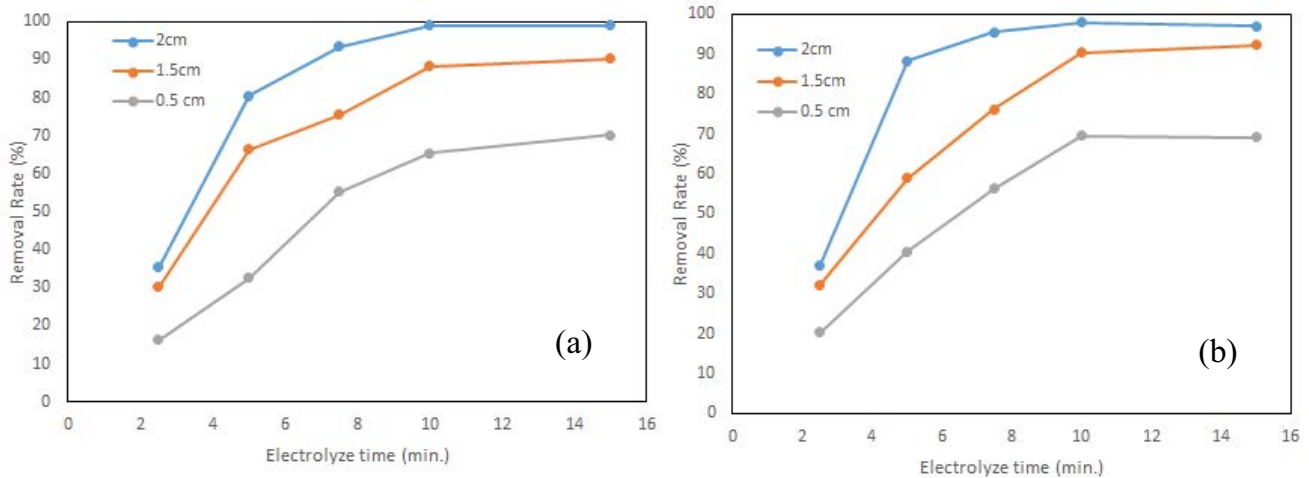


Fig. 9. Effect of distance between the electrodes on (a) color and (b) TOC removal.

Table 4

Current efficiency and operating cost per unit TOC mass after EC treatment of 1 L of DB 60 solution of 100 mg L<sup>-1</sup> using the Al/SS electrode pairs at *j* values ranging between 40 and 100 mA cm<sup>-2</sup>, 25°C

Experiment no.	Energy consumption (kWh m <sup>-3</sup> )	Electrode consumption (kg Al m <sup>-3</sup> )	Operating cost (\$ m <sup>-3</sup> )	Operating cost (\$/kg TOC)	% Current efficiency
1	0.515	0.013	0.060	6.216	102
2	1.538	0.055	0.207	7.898	109
3	2.720	0.134	0.430	16.244	95
4	0.510	0.025	0.081	2.977	97
5	6.695	0.109	0.681	27.157	96
6	0.947	0.034	0.127	6.295	112
7	1.420	0.050	0.191	7.038	116
8	0.553	0.027	0.087	4.609	95
9	4.120	0.067	0.419	19.171	106
Confirmation experiment	3.077	0.109	0.413	15.048	119

of the confirmation experiment is less than some of the trials provided good treatment results for color and TOC removal like runs 3–5 and 9 (Table 3). According to these results, Taguchi experimental design did not provide only the most efficient but also the less expensive solution at the best experimental conditions.

#### 4. Conclusions

This work has demonstrated that EC with Al/SS electrode pairs provided quite good results for the treatment of DB 60. In order to optimize the decolorization of the synthetic wastewater using EC treatment, four variables are considered to determine their optimum levels using Taguchi method. Experiments were conducted to determine the optimum conditions such as initial pH, current density, electrolysis time, and electrical conductivity. According to the results, almost total decolorization 99% and 98% of TOC removal were achieved in 10 min of electrolysis time with the addition of NaCl of 1,000 μs cm<sup>-1</sup> at pH 6 and 80 mA cm<sup>-2</sup>. Operating cost analysis showed that the total cost for EC treatment with

Al/SS electrode pairs to remove TOC from DB 60 solution of 100 mg L<sup>-1</sup> is around 15 US\$ per kg TOC, at the best conditions determined according to Taguchi experimental model.

#### References

- [1] N. Daneshvar, A. Oladegaragoze, N. Djafarzadeh, Decolorization of basic dye solutions by electrocoagulation: an investigation of the effect of operational parameters, *J. Hazard. Mater.*, 129 (2006) 116–122.
- [2] Ö. Gökkuş, Y. Yıldız, Investigation of the effect of process parameters on the coagulation–flocculation treatment of textile wastewater using the Taguchi experimental method, *Fresenius Environ. Bull.*, 23 (2014) 463–470.
- [3] M. Taheri, M.R.A. Moghaddam, M. Arami, Improvement of the/Taguchi/design optimization using artificial intelligence in three acid azo dyes removal by electrocoagulation, *Environ. Prog. Sustainable Energy*, 34 (2015) 1568–1575.
- [4] L. Bilińska, K. Blus, M. Gmurek, S. Ledakowicz, Coupling of electrocoagulation and ozone treatment for textile wastewater reuse, *Chem. Eng. J.*, 358 (2019) 992–1001.
- [5] M. Haddad, S. Abid, M. Hamdi, H. Bouallagui, Reduction of adsorbed dyes content in the discharged sludge coming from an industrial textile wastewater treatment plant using aerobic

- activated sludge process, *J. Environ. Manage.*, 223 (2018) 936–946.
- [6] S. Jorfi, G. Barzegar, M. Ahmadi, R.D.C. Soltani, A. Takdastan, R. Saeedi, M. Abtahi, Enhanced coagulation-photocatalytic treatment of Acid red 73 dye and real textile wastewater using UVA/synthesized MgO nanoparticles, *J. Environ. Manage.*, 177 (2016) 111–118.
- [7] K. Paździór, J. Wrębiak, A. Klepacz-Smółka, M. Gmurek, L. Bilińska, L. Kos, J. Sójka-Ledakowicz, S. Ledakowicz, Influence of ozonation and biodegradation on toxicity of industrial textile wastewater, *J. Environ. Manage.*, 195 (2017) 166–173.
- [8] S.C. Santos, R.A. Boaventura, Treatment of a simulated textile wastewater in a sequencing batch reactor (SBR) with addition of a low-cost adsorbent, *J. Hazard. Mater.*, 291 (2015) 74–82.
- [9] A.A. Babaei, B. Kakavandi, M. Rafiee, F. Kalantarhormizi, I. Purkaram, E. Ahmadi, S. Esmaili, Comparative treatment of textile wastewater by adsorption, Fenton, UV-Fenton and US-Fenton using magnetic nanoparticles-functionalized carbon (MNP@C), *J. Ind. Eng. Chem.*, 56 (2017) 163–174.
- [10] F. Ozyonar, Optimization of operational parameters of electrocoagulation process for real textile wastewater treatment using Taguchi experimental design method, *Desal. Water Treat.*, 57 (2016) 2389–2399.
- [11] B. Palahouane, N. Drouiche, S. Aoudj, K. Bensadok, Cost-effective electrocoagulation process for the remediation of fluoride from pretreated photovoltaic wastewater, *J. Ind. Eng. Chem.*, 22 (2015) 127–131.
- [12] Y.Ş. Yıldız, E. Şenyiğit, Ş. İrdemez, Optimization of specific energy consumption for Bomaplex Red CR-L dye removal from aqueous solution by electrocoagulation using Taguchi-neural method, *Neural Comput. Appl.*, 23 (2013) 1061–1069.
- [13] M. Ahangarnokolaei, H. Ganjidoust, B. Ayati, Optimization of parameters of electrocoagulation/floatation process for removal of Acid Red 14 with mesh stainless steel electrodes, *J. Water Reuse Desal.*, 8 (2017) 278–292.
- [14] Ö. Gökkuş, F. Coşkun, M. Kocaoğlu, Y.Ş. Yıldız, Determination of optimum conditions for color and COD removal of reactive blue 19 by Fenton oxidation process, *Desal. Water Treat.*, 52 (2014) 6156–6165.
- [15] M. Khayet, A. Zahrim, N. Hilal, Modelling and optimization of coagulation of highly concentrated industrial grade leather dye by response surface methodology, *Chem. Eng. J.*, 167 (2011) 77–83.
- [16] T.K. Trinh, L.S. Kang, Response surface methodological approach to optimize the coagulation-flocculation process in drinking water treatment, *Chem. Eng. Res. Des.*, 89 (2011) 1126–1135.
- [17] A. Aleboyeh, N. Daneshvar, M. Kasiri, Optimization of CI Acid Red 14 azo dye removal by electrocoagulation batch process with response surface methodology, *Chem. Eng. Process.*, 47 (2008) 827–832.
- [18] M. Taheri, M.A. Moghaddam, M. Arami, Techno-economical optimization of Reactive Blue 19 removal by combined electrocoagulation/coagulation process through MOPSO using RSM and ANFIS models, *J. Environ. Manage.*, 128 (2013) 798–806.
- [19] N. Daneshvar, A. Khataee, N. Djafarzadeh, The use of artificial neural networks (ANN) for modeling of decolorization of textile dye solution containing CI Basic Yellow 28 by electrocoagulation process, *J. Hazard. Mater.*, 137 (2006) 1788–1795.
- [20] S. Madaeni, S. Koocheki, Application of taguchi method in the optimization of wastewater treatment using spiral-wound reverse osmosis element, *Chem. Eng. J.*, 119 (2006) 37–44.
- [21] D. Ghernaout, A.I. Al-Ghonamy, N. Ait Messaoudene, M. Aichouni, M.W. Naceur, F.Z. Benchelighem, A. Boucherit, Electrocoagulation of direct brown 2 (DB) and BF cibacete blue (CB) using aluminum electrodes, *Sep. Sci. Technol.*, 50 (2015) 1413–1420.
- [22] M. Rivera, M. Pazos, M. Sanromán, Improvement of dye electrochemical treatment by combination with ultrasound technique, *J. Chem. Technol. Biotechnol.*, 84 (2009) 1118–1124.
- [23] M. Kobya, E. Senturk, M. Bayramoglu, Treatment of poultry slaughterhouse wastewaters by electrocoagulation, *J. Hazard. Mater.*, 133 (2006) 172–176.
- [24] APHA, Standard Methods for the Examination of Water and Wastewater, 20th ed., American Public Health Association, Washington, DC, 1998.
- [25] P. Aswathy, R. Gandhimathi, S.T. Ramesh, P.V. Nidheesh, Removal of organics from bilgewater by batch electrocoagulation process, *Sep. Purif. Technol.*, 159 (2016) 108–115.
- [26] J. Lu, Y. Li, M. Yin, X. Ma, S. Lin, Removing heavy metal ions with continuous aluminum electrocoagulation: a study on back mixing and utilization rate of electro-generated Al ions, *Chem. Eng. J.*, 267 (2015) 86–92.
- [27] H.P. de Carvalho, J. Huang, M. Zhao, G. Liu, L. Dong, X. Liu, Improvement of methylene blue removal by electrocoagulation/banana peel adsorption coupling in a batch system, *Alex. Eng. J.*, 54 (2015) 777–786.
- [28] S. Ahmadzadeh, A. Asadipour, M. Pournamdari, B. Behnam, H.R. Rahimi, M. Dolatabadi, Removal of ciprofloxacin from hospital wastewater using electrocoagulation technique by aluminum electrode: Optimization and modelling through response surface methodology, *Process Saf. Environ. Prot.*, 109 (2017) 538–547.
- [29] M. Kobya, E. Demirbas, Evaluations of operating parameters on treatment of can manufacturing wastewater by electrocoagulation, *J. Water Process Eng.*, 8 (2015) 64–74.
- [30] R. Katal, H. Pahlavanzadeh, Influence of different combinations of aluminum and iron electrode on electrocoagulation efficiency: application to the treatment of paper mill wastewater, *Desalination*, 265 (2011) 199–205.
- [31] W. Mook, M. Aroua, M. Szlachta, C. Lee, Optimisation of reactive black 5 dye removal by electrocoagulation process using response surface methodology, *Water Sci. Technol.*, 75 (2016) 952–962.
- [32] H. Zazou, H. Afanga, S. Akhouairi, H. Ouchtak, A.A. Addi, R.A. Akbour, A. Assabbane, J. Douch, A. Elmchaouri, J. Duplay, Treatment of textile industry wastewater by electrocoagulation coupled with electrochemical advanced oxidation process, *J. Water Process Eng.*, 28 (2019) 214–221.
- [33] B.K. Nandi, S. Patel, Effects of operational parameters on the removal of brilliant green dye from aqueous solutions by electrocoagulation, *Arabian J. Chem.*, 10 (2017) S2961–S2968.
- [34] L. Shamaei, B. Khorshidi, B. Perdicakis, M. Sadrzadeh, Treatment of oil sands produced water using combined electrocoagulation and chemical coagulation techniques, *Sci. Total Environ.*, 645 (2018) 560–572.
- [35] F. Ozyonar, Treatment of train industry oily wastewater by electrocoagulation with hybrid electrode pairs and different electrode connection modes, *Int. J. Electrochem. Sci.*, 11 (2016) 1456–1471.
- [36] F. Ozyonar, B. Karagozoglu, Investigation of technical and economic analysis of electrocoagulation process for the treatment of great and small cattle slaughterhouse wastewater, *Desal. Water Treat.*, 52 (2014) 74–87.
- [37] M. Ahmadi, F. Ghanbari, Optimizing COD removal from greywater by photoelectro-persulfate process using Box-Behnken design: assessment of effluent quality and electrical energy consumption, *Environ. Sci. Pollut. Res.*, 23 (2016) 19350–19361.
- [38] F. Ghanbari, M. Moradi, A. Mohseni-Bandpei, F. Gohari, T.M. Abkenar, E. Aghayani, Simultaneous application of iron and aluminum anodes for nitrate removal: a comprehensive parametric study, *Int. J. Environ. Sci. Technol.*, 11 (2014) 1653–1660.
- [39] C.J. Izquierdo, P. Canizares, M. Rodrigo, J. Lederc, G. Valentin, F. Lapique, Effect of the nature of the supporting electrolyte on the treatment of soluble oils by electrocoagulation, *Desalination*, 255 (2010) 15–20.
- [40] C.A. Martínez-Huitle, E. Brillas, Decontamination of wastewaters containing synthetic organic dyes by electrochemical methods: a general review, *Appl. Catal., B*, 87 (2009) 105–145.
- [41] G. Chen, Electrochemical technologies in wastewater treatment, *Sep. Purif. Technol.*, 38 (2004) 11–41.
- [42] A.K. Golder, A.N. Samanta, S. Ray, Removal of Cr<sup>3+</sup> by electrocoagulation with multiple electrodes: bipolar and monopolar configurations, *J. Hazard. Mater.*, 141 (2007) 653–661.